Sustainable Energy, Grids and Networks 39 (2024) 101489

Contents lists available at ScienceDirect

Sustainable Energy, Grids and Networks

journal homepage: www.elsevier.com/locate/segan

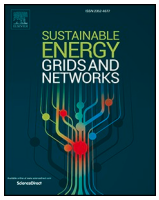

Coordination of solar battery hybrid power plants and synchronous generators for improving black start capability

Michael Beck, M.J. Hossain *

School of Electrical and Data Engineering, University of Technology Sydney, NSW 2007, Australia

ARTICLE INFO

Keywords:
Hybrid energy
Hybrid power plant
Black start
Integration of renewable energy
Synchronous generation

ABSTRACT

Renewable generation utilizes inverter-based technology which is much different than the coal and nuclear synchronous machines it is replacing. The electrical network was designed around big synchronous machines providing constant dispatchable power and innate inertia to dampen frequency disturbances. The network protection system is based on high available fault current provided by the big generators. The renewable plants have a variable fuel supply, no inertia, and provide less fault current for system protection. A hybrid power plant with renewables, energy storage, and a synchronous generator can play a significant role in restoring power system operation after the occurrence of a blackout. This paper presents an improved method to utilize inverter-based resources (IBR) with existing synchronous generation to improve the black start capability while minimizing the overall system's operation cost and providing additional ancillary grid services. A battery energy storage system is modeled with grid forming inverters to provide black start to the synchronous unit while the solar is modeled with grid following inverters. A Long-Short Term Memory (LSTM) is developed to model the auxiliary load for reducing the fuel consumption in synchronous generators and reducing the cost. Several case studies are conducted to verify the performance of the grid forming inverters with battery storage to start the largest direct online (DOL) and soft start motors. Utilizing actual synchronous generator auxiliary load data for a year, a quasi-dynamic simulation analysis is performed to determine energy storage requirements for black start. Finally, the energy benefits of the solar installation are estimated from simulating the hybrid system for 1 year. A reduced fuel burn simulation is performed by constraining the export power to the actual data and reducing synchronous generation to account for the solar generation and the reduced auxiliary load. The study finds that the IBR resources are capable of successfully black starting the synchronous generator and reducing fuel consumption and earning additional revenue from the solar plants.

1. Introduction

Traditional large synchronous machine power plants provide the electric grid with dispatchable power and ancillary services such as frequency regulation and voltage regulation needed for a secure and reliable network. As these plants are retired, they are being replaced by modern technology renewable energy power plants [1]. These plants are non-synchronous inverter-based technology plants which are non-controllable and intermittent in nature. The inverter-based generators are not capable of providing the same level of frequency and voltage regulation. This has caused many challenges for grid operators to maintain system integrity [2]. A solution to provide dispatchable power from renewable resources is to combine multiple renewable energy sources with energy storage [3]. Another possibility is to integrate new renewable generation with synchronous generators at the plant level. Currently, there is limited research and development in this area. This would provide an increase in the use of renewables as well as reduction in the synchronous plant fuel usage which could be fossil fuel. The synchronous generator would provide inherent inertia and regulatory services to the grid. The coordination of all these devices can contribute to improving black start capability.

Australia has taken the lead in installing battery storage at fossil fuel plants. AGL is planning to add 150 MW, 1 hour battery storage at its Liddell coal generation station, 250 MW, 1 hour battery storage at its Torrens Island gas generation station, and a 200 MW, 4-hour battery at its Loy Yang coal generation station. Energy Australia announced its plans to add a 350 MW, 4-hour battery bank at its Yallourn coal generation station. Origin Energy plans to build a 700 MW, 4 hour battery

* Corresponding author.
E-mail addresses: Michael.beck@student.uts.edu.au (M. Beck), Jahangir.hossain@uts.edu.au (M.J. Hossain).

https://doi.org/10.1016/j.segan.2024.101489
Received 15 November 2023; Received in revised form 18 June 2024; Accepted 26 July 2024
Available online 2 August 2024

installation at its Eraring Power Station [4]. The Torrens Island installation will utilize grid forming inverters [5]. However, all these battery installations will be separate, independently operated resources.

In 2017, a novel proposal to add a 46 MW solar photovoltaic resource addition to the existing IPP4-Jordan 250 MW tri-fueled power plant was developed by diesel engine manufacturer Wartsila [6]. The solar plant would have connected to the existing generation station's 15 kV MV network. The solar energy would supply the plant auxiliary load and any excess would be exported to the grid through the site's main transformer. During the day when the photovoltaic power plant would be generating at nameplate, the thermal plant's heat rate would be improved by 18.4 %. However, the project was not constructed. Instead, a 52 MW solar power plant was constructed at the site with a separate connection to the 132 kV transmission network and a separate power purchase agreement (PPA) with National Electric Power Company (NEPCO) [7].

Existing research predominantly explores the application of IBRs for black start capabilities within IBR-only microgrids [8,9]. Notably, the NREL has conducted research on utilizing IBRs for grid black starting [10]. Initial investigations by the NREL encompassed modeling four distinct network configurations regarding the integration of IBRs into the grid. However, the scope of performance validation was confined to initiating a single standard squirrel cage induction motor.

Subsequent NREL research delves into the control of network IBR resources for grid restart purposes [11] [12]. A significant challenge with this is that different entities own and operate the various resources on the network. This requires a great deal of coordination. The controls and equipment at remote sites will require a great deal of modification to coordinate starting a remote synchronous generating plant. One key advantage of this paper's proposed approach lies in its utilization of an actual synchronous generating plant and associated equipment, thereby enabling a more realistic simulation. This simulation not only assesses motor starting performance but also evaluates the synchronization of a large generator with a microgrid powered by IBRs.

Several current studies focus on the energy management control of microgrids. In [13] and [14], the authors utilize a DC microgrid as the basis for their energy management control. In modelling and analyses, the grid energy is considered to be constant in [13,14]. In a real black start situation, this would not be the case. Further investigation is required to determine the applicability of the proposed energy management system to black starting a synchronous generator in real grid operating conditions. Another recent paper [15] proposes an adaptive coordinated energy management of various IBR resources including energy storage. The method only includes DC coupled IBR resources. The model used for simulation does not include synchronous machine generators or motors. However, still large parts of existing generators are synchronous machines. Limited analyses have been conducted in the literature to show how to utilize synchronous generators with IBRs to improve the black start capability of the grid.

A very detailed energy management system for a hybrid AC/DC microgrid is presented in [16]. The authors describe a 2-layer control strategy to maintain the microgrid's stability. The research in our paper focuses on building a temporary microgrid during a network black-out, with the objective of re-starting the main synchronous generator. Once on-line, the synchronous generator can be utilized to start energizing the wider transmission network. Additional research has been conducted on the topic of using grid forming inverters on solar plants to provide black-start capability [17]. This could be utilized in network restoration. Due to the length of time (24 hours) required to bring the coal fired generation on-line, grid forming solar was not considered. Instead, grid forming BESS is utilized with grid following solar providing supplemental energy. Most research today focuses on complete replacement of synchronous plants with IBR. This is a step change from the modern power network and as such, requires significant modifications and investment to implement. The strategy presented in this paper takes an incremental approach to integrating IBR with the modern grid. It utilizes an existing generation resource and hybridizes it with new IBR technology resulting in a new generation resource with additional capability and improved efficiency.

The novelty of this research methodology lies in its holistic evaluation of the performance and advantages of employing IBRs for restarting a significant synchronous generator during blackout scenarios. The study verifies dynamic performance, delineates energy requirements, and assesses the economic benefits for generation owners

As an increasing number of IBR power plants are being brought online, synchronous generators are being retired, leading to grid stability concerns arising from the loss of inertia. The primary objective of this research is to illustrate the advantages of a unique implementation of IBR directly into existing synchronous generation facilities. The key goals include showcasing black start capability, enhancing renewable energy output, ensuring sustained system inertia, and reducing reliance on fossil fuels. While prior studies have concentrated on enhancing grid stability by augmenting IBR at the expense of synchronous generation, this research adopts a novel perspective by integrating IBR with existing synchronous machines to uphold network stability.

This research will model and simulate integration of solar power and battery to existing fossil fuel power plant to reduce fuel burn and provide black-start capability. A LSTM model is developed to accurately model the auxiliary load to reduce the cost and improve the energy efficiency. Several case studies are conducted with grid forming battery inverter and grid following solar inverter to show the capability of proposed coordinated IBR and synchronous generators for proving black start capability after the system blackout.

The rest of the paper is organized as follows. Section 2 details the existing synchronous plant model and describes the model development of the solar/battery installation. The PV is modeled with grid following (GFM) inverters while the BESS uses grid forming (GFM) inverters to maintain the microgrid during unit black start. Section 3 describes the methodology used to demonstrate integration of the solar/BESS installations with the synchronous generator. The methodology encompasses both the dynamic power requirements as well as the long-term energy requirements. The simulations use real data from the generation site. Section 4 will detail the results from the case study simulations. This includes dynamic responses during large motor starts and synchronizing of generator to the BESS supported microgrid. It also shows the BESS energy requirements for providing black start and estimates the reduced fuel burn provided by the addition of PV generation. Finally, Section 5 concludes the findings of this paper.

2. Modelling

The system under consideration consists of synchronous generator, solar PV systems, battery energy storage systems and loads. Their modeling is discussed below.

2.1. Existing plant model

The existing fossil fuel power station selected for this study is in the United States. It is comprised of four 600 MW steam driven synchronous generators. Each generator has a terminal voltage of 21 kV. Each generator has a separate generation step up transformer to connect to the 230 kV network. The auxiliary load of each unit is supplied by 21 kV/6.9 kV transformers. The generating units synchronize to the network at the 230 kV bus. Because of this, each unit also has a 230 kV/6.9 kV unit start-up transformer to provide auxiliary load until the generator syncs. Units 1 & 2 have interties on the 6.9 kV as do units 3 & 4 for contingencies. The IEEEG1 model [18] is used to represent the turbine generator governor. The IEEE ST4B [19] standard exciter model represents the synchronous generator exciter, and the IEEE PSS2A [20] is utilized for the power system stabilizer. All parameters are taken from the existing generating unit modelling data.

2.2. Solar/battery model

Two separate solar/battery plants are proposed to have redundancy in the system. The solar plants are sized to maximize power output while utilising the existing 6.9 kV network. The battery bank power rating is also sized to maximize charging capability and supply maximum power to auxiliary systems during black start. The battery storage is lithium-ion technology with an assumed 2 % self-discharge per month [21]. The controller maintains the state of charge (SOC) between 70 % and 90 % while unit is grid connected. During a grid outage, the SOC is allowed to be between 10 % and 100 %. The renewables will tie into the existing electrical infrastructure on the 6.9 kV auxiliary load network. The rating of the existing switchboards and breakers is 3000 Amp (@35 MW at 6.9 kV). This study proposes a connection on each of the two 6.9 kV switchboards. This will put one renewable infeed on each auxiliary transformer low side network. The solar farm will consist of two separate fields each rated at 35 MW AC. During daylight hours, this can supply power for all the auxiliary load required by Units 3 and 4 during full generation by both units. To reduce losses and conductor size, the AC will be transformed to 34.5 kV and connected to the new 34.5 kV network. A 34.5 kV/6.9 kV transformer will connect the renewable power to the Unit 4 6.9 kV network. The PV plant will be connected to the 690 V AC bus through separate non-grid forming inverters. The battery will be sized to supply auxiliary load needed to black start the unit from a cold start and be connected to the 690 V AC bus through grid forming converters. The unit start-up transformer will be utilised to provide 230 kV voltage for the unit to sync. The auxiliary load from the other 3 units can be used to increase the unit load until the network can be rebuilt and additional external load can be brought online.

This study is focused on utilising grid forming (GFM) converters with battery storage to black start a synchronous generator. In all dynamic simulations, the PV plant inverters are disconnected from the network and can be disregarded. The PV plant is only considered during the Quasi-dynamic energy simulations. The PV plant equipment uses available manufacturer nameplate data for the solar panels, inverters, and transformers.

The following equations are used to model PV plant output [22]:

$$P_{pvplant} = P_{panel} \bullet num_{panels} \tag{1}$$

$$P_{panel} = \frac{E_{g.pv} \bullet P_{pk.panel} \bullet \eta_{rel} \bullet \eta_{inv}}{E_{STD}} \tag{2}$$

Where:

- P_{panel}=active power output of each panel
- $P_{pvplant}$=PV plant active power output
- num_{panels}=number of panels per inverter
- $E_{g.pv}$=global irradiance on the plane of the array
- E_{STD}=standard irradiance ($1000 W/m^2$)
- $P_{pk.panel}$=rated panel peak power
- η_{rel}=relative panel efficiency
- η_{inv}=inverter efficiency

The grid forming control droop equations are [23]:

$$\Delta\omega_{droop} = m_p \Delta p_{LPF} \tag{3}$$

$$\Delta v_{droop} = m_q \Delta q_{LPF} \tag{4}$$

Where $\Delta\omega_{droop}$ is the frequency deviation and Δv_{droop} is the voltage deviation from load flow initialization. m_p and m_q are the active and reactive droop coefficients, and Δp_{LPF} and Δq_{LPF} are the power deviations from load flow initialization. As shown in Figs. 1 and 2, the real and reactive power measured at the grid interphase is low pass filtered to stabilise the control loops during power measurement oscillations.

The converter model utilises a virtual impedance controller to improve transient load sharing during synchronization and parallel operation with the generator during black start operations. The controller is based on [24]. The voltage drop (real $\Delta u_{vi,r}$, reactive $\Delta u_{vi,i}$) across the virtual impedance is:

$$\Delta u_{vi,r} = r_{vi} i_{vi,r} - x_{vi} i_{vi,i} \tag{5}$$

$$\Delta u_{vi,i} = r_{vi} i_{vi,i} + x_{vi} i_{vi,r} \tag{6}$$

where r_{vi} and x_{vi} are the resistance and reactance of the virtual impedance. i_{vi} is the converter current. The virtual impedance controller adjusts the parameters according to grid conditions. The impedance is adjusted when the current exceeds the set threshold $i_{\lim}$as shown:

$$z_{vi} = \begin{cases} r_{vi} + jx_{vi} if |i_{vi}| \le i_{\lim} \\ (k_{pr} r_{vi} + jk_{px} x_{vi})(|i_{vi}| - i_{\lim}) + r_{vi} + jx_{vi} otherwise \end{cases} \tag{7}$$

k_{pr} and k_{px} are proportional factors for the virtual resistor and reactance.

2.3. Primary air fan motor model

The largest DOL motor start required during a unit run up is the primary air (PA) fan motor. The motor is a 6.6 kV, 1268 kW, 4 pole motor. The moment of inertia is $443 kgm^2$ with an acceleration time constant of 12.32 seconds. The motor connects to the 6.9 kV auxiliary load bus by 481 m 500 MCM cooper cables.

2.4. Induction air fan motor model

The largest motor start required during a unit run up is the induced draft (ID) fan motor. The motor is a 6.6 kV, 7271 kW, 10 pole motor. The moment of inertia is 46,201 kg mˆ2 with an acceleration time constant of 35.92 seconds. The motor is powered by an 8200 kW 6.9–6.6 kV VFD. The VFD connects to the 6.9 kV auxiliary load bus by 1106 m 4×750 MCM cooper cables. The installed VFD can start and run the motor at any speed from 0.01 pu to 1 pu.

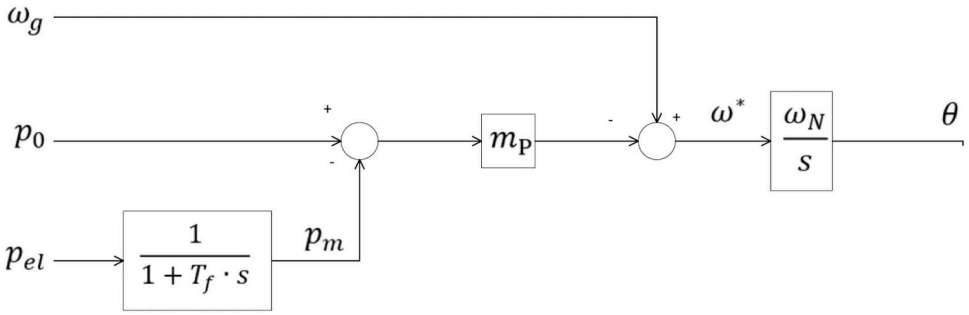

Fig. 1. Frequency droop control.

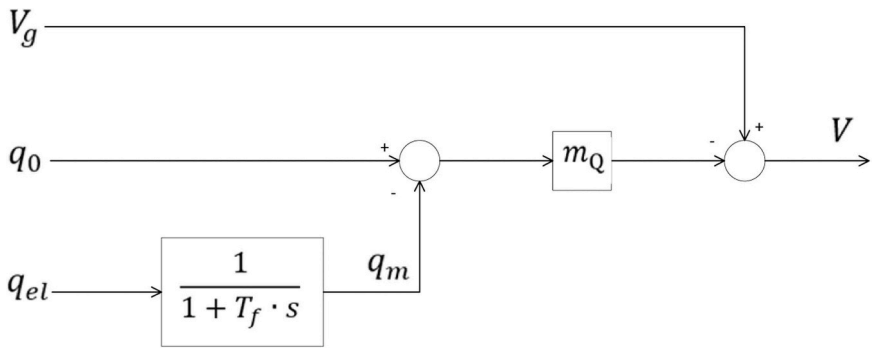

Fig. 2. Voltage droop control.

3. Proposed black start method

Providing black start capability to the synchronous generator requires the auxiliary plant network to be operated as a microgrid island. The microgrid requires adequate dynamic response to load changes and adequate energy reserves to provide the necessary auxiliary load for the unit to start up. Finally, during normal operation, the added energy resources should reduce the plant fuel consumption. Fig. 3 lays out the overall study methodology.

Current research into utilizing IBR for black start generally falls into two categories. The first is the network solution methodology [25]. This requires remote IBR resources to provide power and dynamic support to the synchronous plant auxiliary loads and generator synchronization. In the modern power system, these resources are likely to be owned and operated by unique entities. The IBR control systems are not tuned to specific large motor starts required as part of the synchronous unit start-up. They will also need to provide frequency and voltage support as the large generator syncs to the grid. The methodology proposed in this paper utilizes the PV and BESS to augment the capabilities of the existing synchronous generator. The control and operation of the PV and BESS assets will coordinate with the synchronous generator black start requirements as a primary function. The second category is the 100 % renewable microgrid methodology [26]. This considers black starting individual microgrids and then building the grid back by interconnecting the multiple microgrids. This research does not consider the intricacies of starting a large synchronous generator. It is focused on 100 % renewable energy grids.

The proposed microgrid is powered by GFM inverter connected BESS and GFL inverter connected photovoltaic plants. The microgrid must be operated such that at steady state:

$$S_{solar} + S_{battery} + S_{synchronous\ generator} - S_{aux\ load} - S_{network\ losses} \cong 0$$

$$f \cong 1pu \tag{8}$$

$$v \cong 1pu$$

The GFM droop control is tuned to dampen voltage and frequency transients created during network disturbances like large motor starts and in the most extreme case, synchronizing the generator unit to the microgrid.

The BESS must be adequately sized to provide energy for the auxiliary loads needed for the duration of unit startup with the battery state of charge (SOC) constrained by a min and max level, i.e.:

$$E_{battery} + E_{solar} \geq E_{aux\ load} + E_{network\ losses} \tag{9}$$

$$\min soc \leq SOC \leq \max soc$$

The complete algorithm is detailed in Fig. 4.

The point of connection (POC) energy export of the synchronous power plant is:

$$E_{POC} = E_{synchronous\ generator} - E_{aux\ load} - E_{network\ losses} \tag{10}$$

The additional energy provided by the renewable integration is:

$$-E_{battery} + E_{solar} \tag{11}$$

Constraining P_{POC} to the original dispatch value and allowing $P_{synchronous\ generator}$ to vary constrained by minimum generation and neglecting changes in network losses and auxiliary load:

$$P_{reduced\ synchronous\ generation} = P_{synchronous\ generator} - P_{solar} \tag{12}$$

The details of the algorithm are shown in Fig. 5.

To improve accuracy of the energy/reduced fuel benefits calculations, a long short-term memory (LSTM) network is developed utilizing the auxiliary load and generation data. The LSTM uses the generator MW [G], temperature [T], day of week [d], and hour of day [h] as inputs into the LSTM as shown in Fig. 6. The total auxiliary power [A] is the target. The LSTM model is set up with 1 layer and 64 nodes with a 1-hour (n=60) lookback. The LSTM training uses the first 90 % of data to train the model with the last 10 % utilized to test. The training runs 1000 epochs with a learning rate of 0.0001. The training calculates a validation loss of each epoch. The epoch model with the lowest validation loss is selected as the model to predict the test data. The LSTM model proved a good predictor of the test data. It had an MSE of 2.04 and an R^2 score of 0.98.

The actual generation data is replaced with the reduced synchronous generation data [G*] and utilizing the LSTM model, predicted total auxiliary load data [A*] is output. Each of the auxiliary loads is calculated utilizing the original data load proportions. The reactive load and generation are calculated using the original data power factors. The LSTM regressed reduced aux load data is used along with the previously calculated reduced synchronous generation to calculate the new E_{POC}.

$$E_{new\ POC} = E_{reduced\ synchronous\ generator} - E_{\ reduced\ aux\ load} - E_{network\ losses} - E_{battery} + E_{solar} \tag{13}$$

The energy benefits and fuel reduction benefits are:

$$E_{new\ POC} - E_{POC} \tag{14}$$

$$E_{synchronous\ generator} - E_{reduced\ synchronous\ generation} \tag{15}$$

4. Results and discussions

The single line diagram of the test system is shown in Fig. 7. A successful start of the coal fired generating unit requires a temporary microgrid that can power the auxiliary load of the unit and maintain stability. The most disruption to the stability of the microgrid occurs during large induction motor starts and the synchronization of the generator to the temporary microgrid. The first case study simulates starting of the 2 largest motors needed for the unit to start. This shows the dynamic performance of the IBR for large load pick up. The second case study simulates the dynamic performance of the IBR during the unit synchronization. Another requirement of a successful black start is meeting the unit startup energy requirements. The next case study

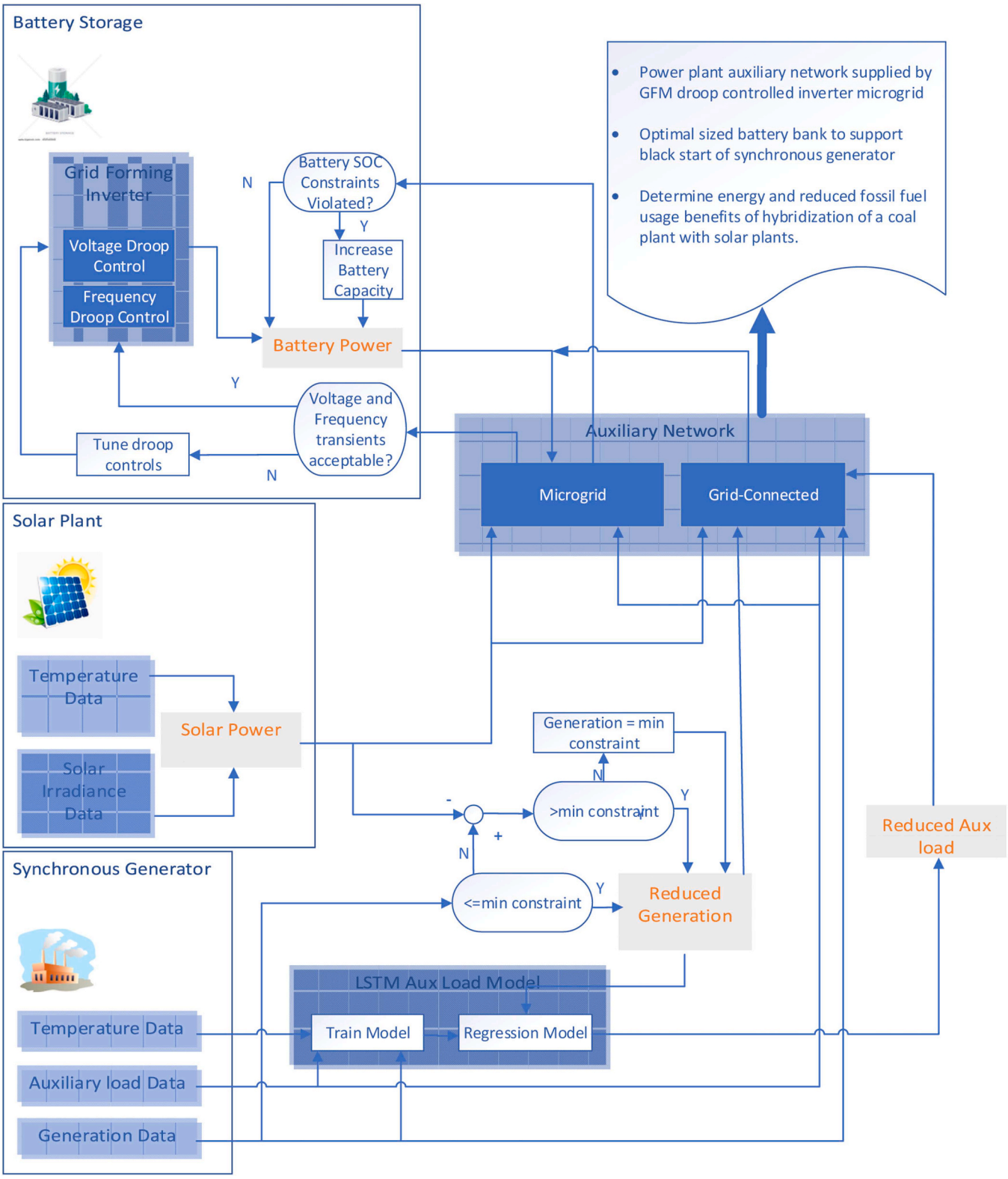

Fig. 3. Study methodology.

simulates the 24-hour loading experienced during a cold unit start-up using auxiliary load data from a previous unit start. This is used to determine the size of battery storage needed to supply auxiliary load during a unit start. Finally, a successful black start methodology must provide additional economic and environmental benefits. The final case study uses the actual 1-year generation and auxiliary load data to simulate increased generation capacity and potential reduction in fossil fuel usage.

4.1. Case study-grid forming inverter for starting motors

4.1.1. PA (primary air) fan motor start

The system model is configured with the synchronous generator off, and auxiliary loads being supplied from the grid forming inverters. This

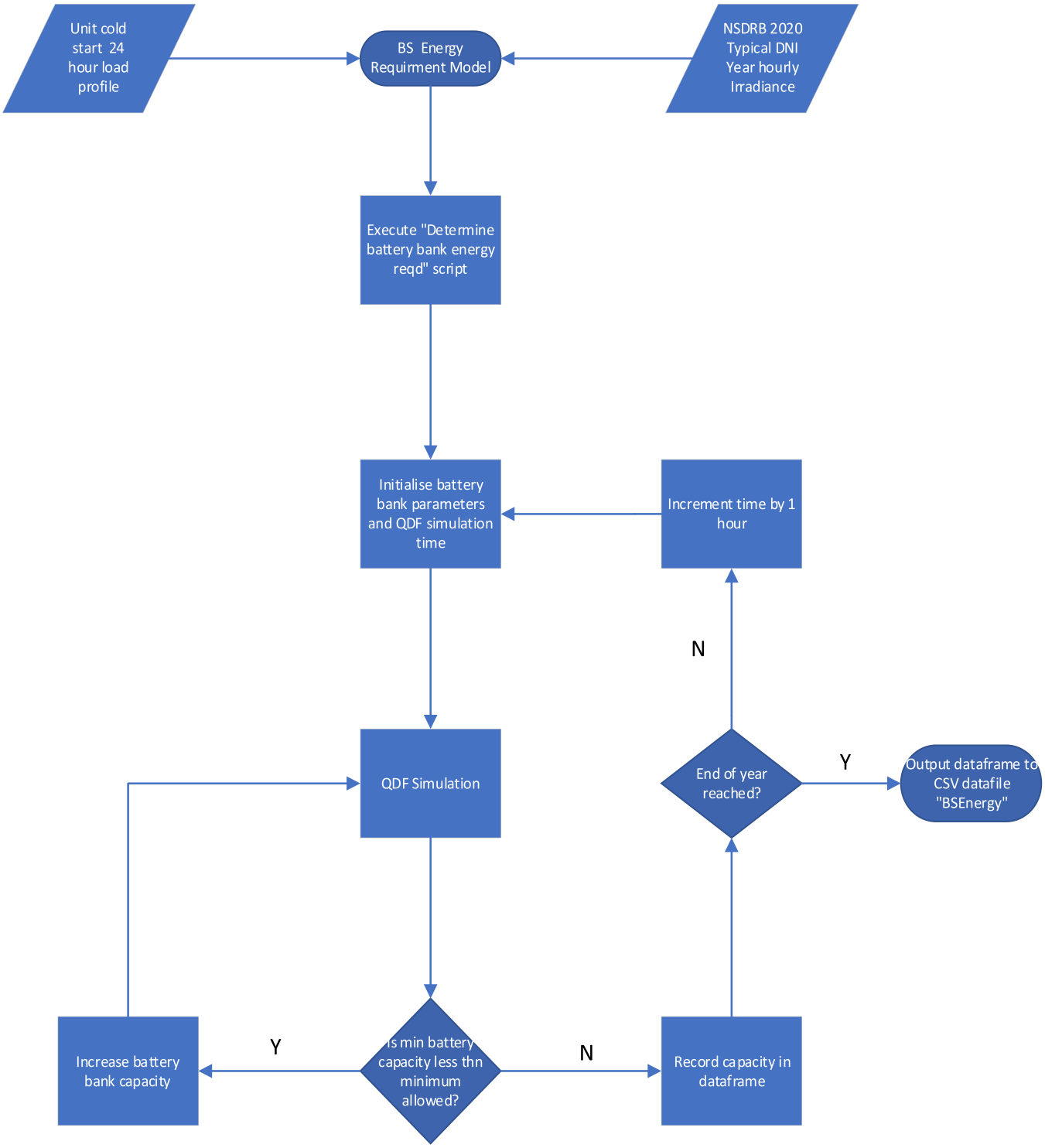

Fig. 4. Black start energy capacity requirement simulation logic.

simulation is to test the ability of the grid forming converters to successfully start the motor. To simplify the simulation, the solar grid following inverters are disconnected as well. The two auxiliary bus loads are set at the maximum values seen during a startup (9 MW and 7.5 MVAR). The bus tie between the two 6.9 kV auxiliary buses is closed. An EMT (electromagnetic transient) simulation is run for 30 s with a 0.0001 s integration step size. At t=3 s, the 6.9 kV breaker feeding the PA fan motor is closed.

The PA fan motor start simulation results shown in Fig. 8 indicate a successful motor start by achieving rated speed in 16.5 s. The grid forming converters only see a maximum 0.014 pu drop in voltage. At the time of breaker closing, the frequency sees a maximum oscillation from 0.99 pu to 1.01 pu but returns to steady state within 0.03 seconds.

4.1.2. ID (induced draft) fan motor start

The VFD (variable frequency draft) greatly reduces the loading on the converters to start the ID Fan. Since the VFD allows gradual loading of the motor, a minimal speed of 0.02 pu is selected to simulate the start-up. Once the motor is started, its speed can gradually be increased without a significant impact to the converters. The system model is

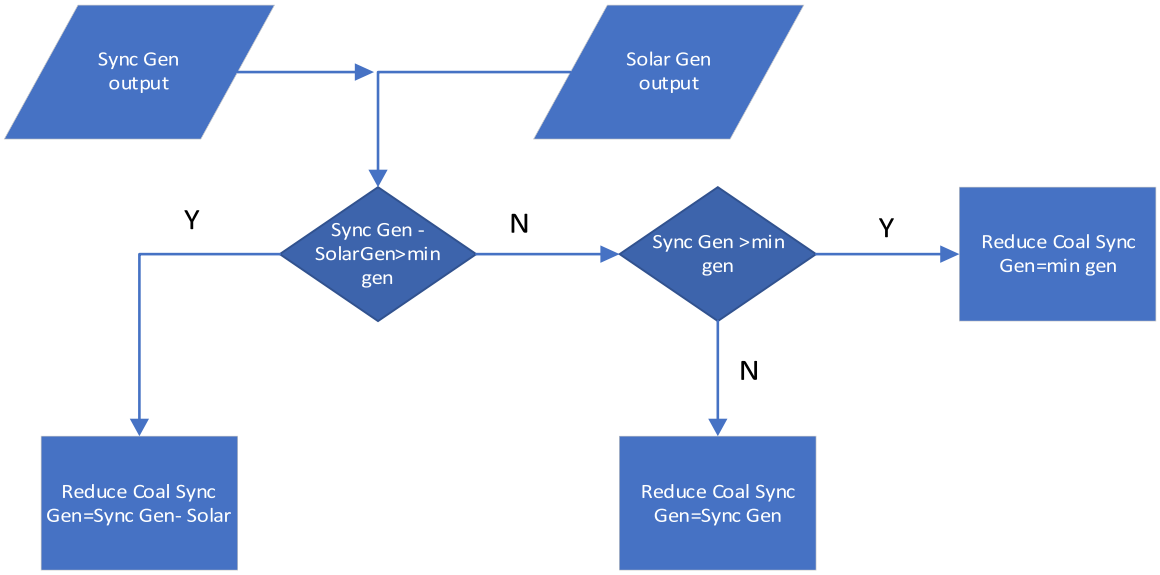

Fig. 5. Reduce coal fuel logic.

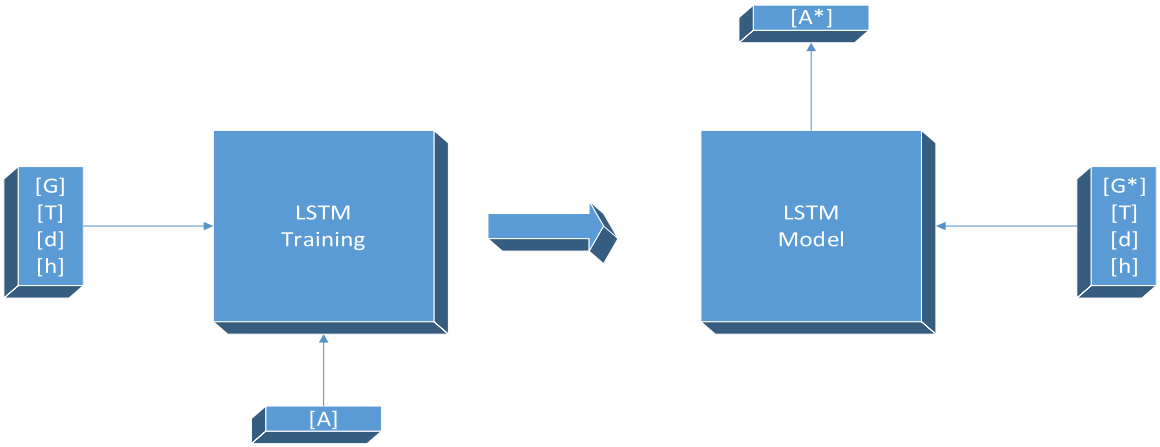

Fig. 6. LSTM model.

configured with the synchronous generator off with the auxiliary loads isolated from the auxiliary and start up transformers and being supplied from the grid forming inverters. This simulation is to test the ability of the grid forming converters to successfully start the motor. To simplify the simulation, the solar grid following inverters are disconnected as well. The two auxiliary bus loads are set at the maximum values seen during a startup (9 MW and 7.5 MVAR). The bus tie between the two 6.9 kV auxiliary buses is closed. An EMT simulation is run for 20 s with a 0.0001 s integration step size. The VFD speed is set to 0.02 pu. At t=2 s, the VFD receives a start command. The VFD closes in, and the motor begins accelerating until it reaches 0.02 pu speed.

The ID fan motor start simulation results shown in Fig. 9 indicate a successful motor start by achieving a stable 0.0194 pu speed in 20 s. The grid forming converters see a minimum.93 pu and maximum 1.046 pu fluctuation at breaker closing lasting 0.011 s. The frequency is stable at VFD energization with a slight oscillation. The oscillations may be removed or reduced through further VFD harmonic filter and grid forming converter tuning.

4.2. *Case study for synchronizing generator with grid forming inverter*

The system model is configured with the synchronous generator on and spinning at synchronous speed. The 230 kV breaker connecting the generating station transformer (GSU) is opened. The auxiliary transformers are disconnected and the microgrid is connected to the 230 kV island through the two start up transformers. Synchronization of the generator with the microgrid occurs when the GSU high side breaker closes in. This simulation is to test the ability of the grid forming converter microgrid to successfully sync with the existing synchronous generator. To simplify the simulation, the solar grid following inverters are disconnected. The two auxiliary bus loads are set at the maximum values seen during a startup (9 MW and 7.5 MVAR). An EMT simulation is run for 4 s with a 0.0001 s integration step size. The GSU high side breaker closes at t=2 s connecting the synchronous generator to the microgrid.

The generator synchronization simulation indicates a successful synchronization of the generator to the microgrid. The converter voltage oscillations at switching range from 1.01 to 1.055 pu and stabilize in 0.5 seconds (Fig. 10). The frequency oscillations range from 0.971 to 1.041 pu and stabilize in 0.2 seconds (Fig. 11). Each converter sees a spike in current to 2 pu which dampens down to steady state in 0.3 seconds (Fig. 12). When the generator syncs, it initially slows down from 1 pu to 0.9987 pu in 0.25 seconds. This loss of inertia results in generator output. As seen from Fig. 13, the converters absorb the generator's inertial energy.

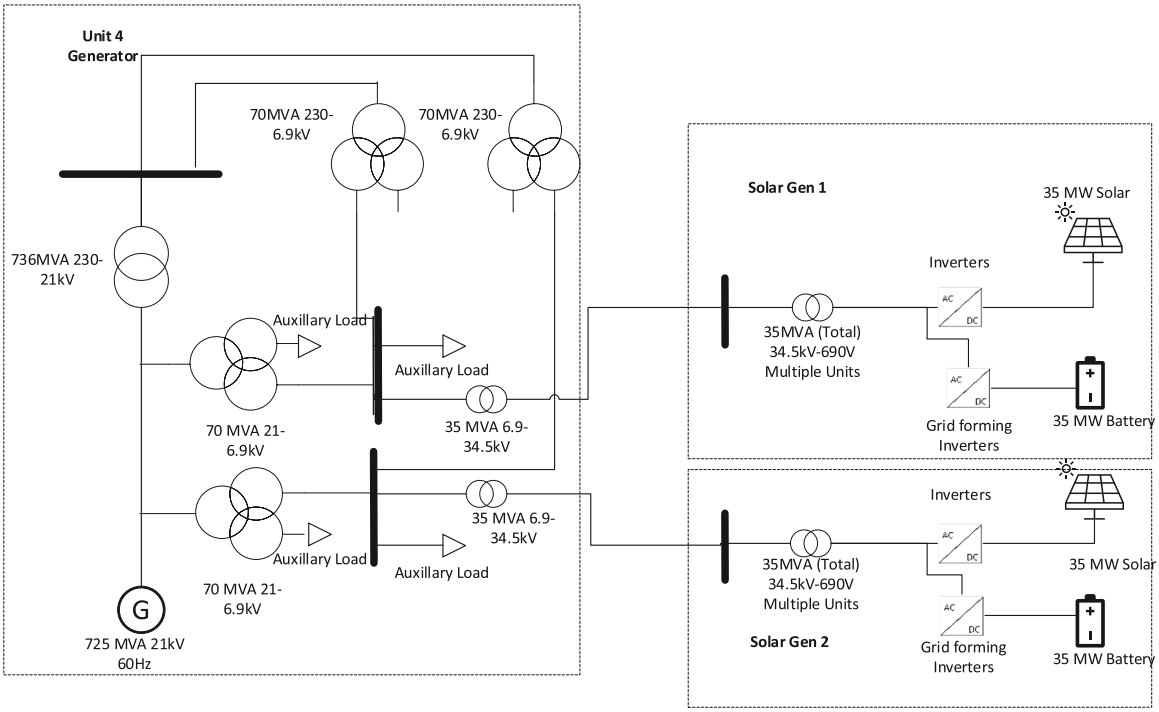

Fig. 7. Single line diagram of the plant model.

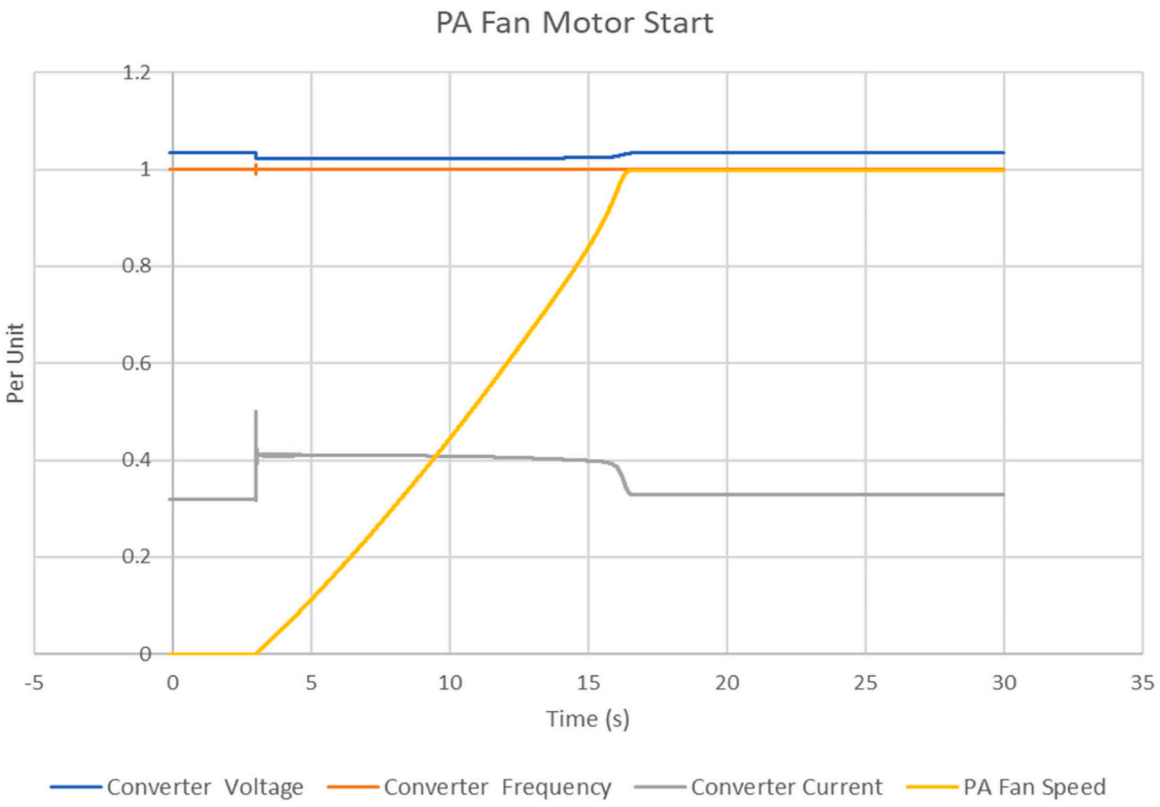

Fig. 8. PA fan motor start simulation results.

4.3. Case study for determining black start energy requirements

The system model is configured with the synchronous generator off. The 230 kV breaker connecting the generating station transformer (GSU) is opened. The auxiliary transformers are disconnected and the microgrid is connected to the 230 kV island through the two start up transformers. The purpose of this simulation is to determine energy storage requirements for starting up the synchronous generator.

The quasi-dynamic simulation utilizing the python script (Fig. 4) shows each battery plant would need to be 235 MWhr to be capable of

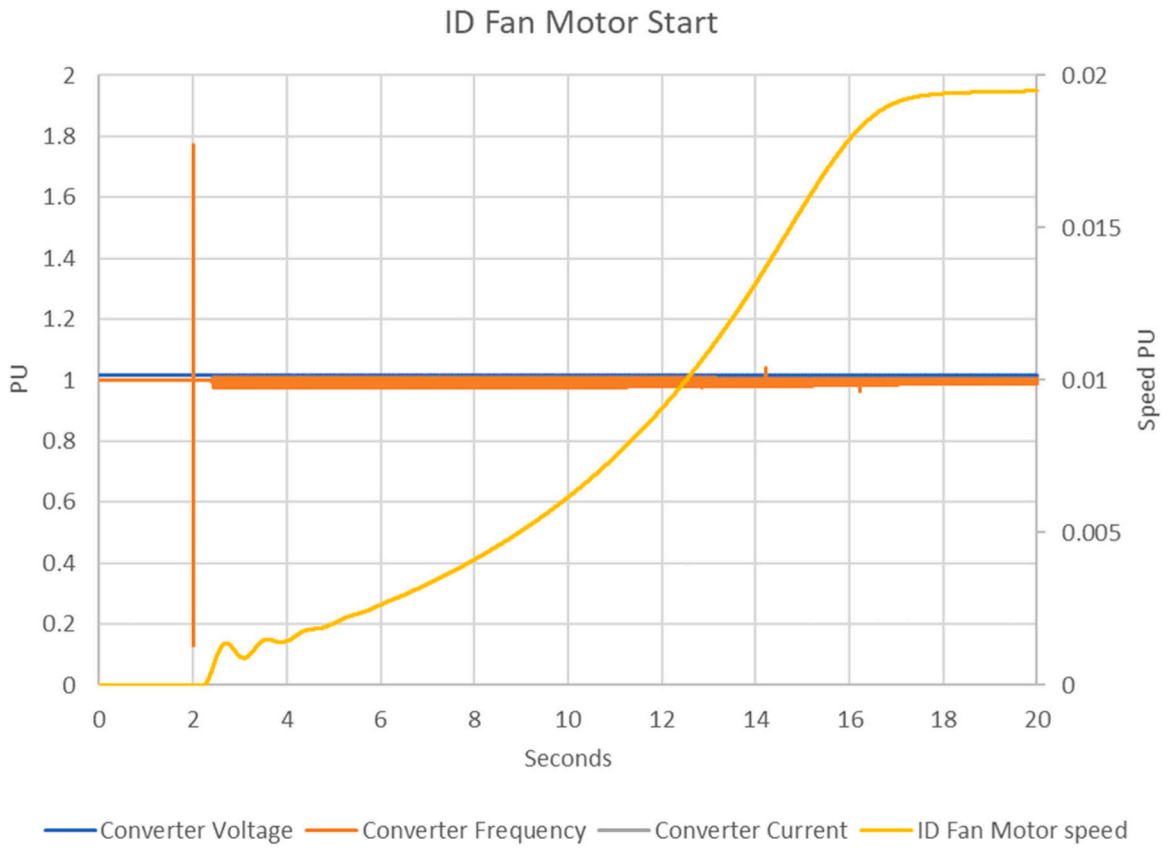

Fig. 9. ID fan motor start simulation results.

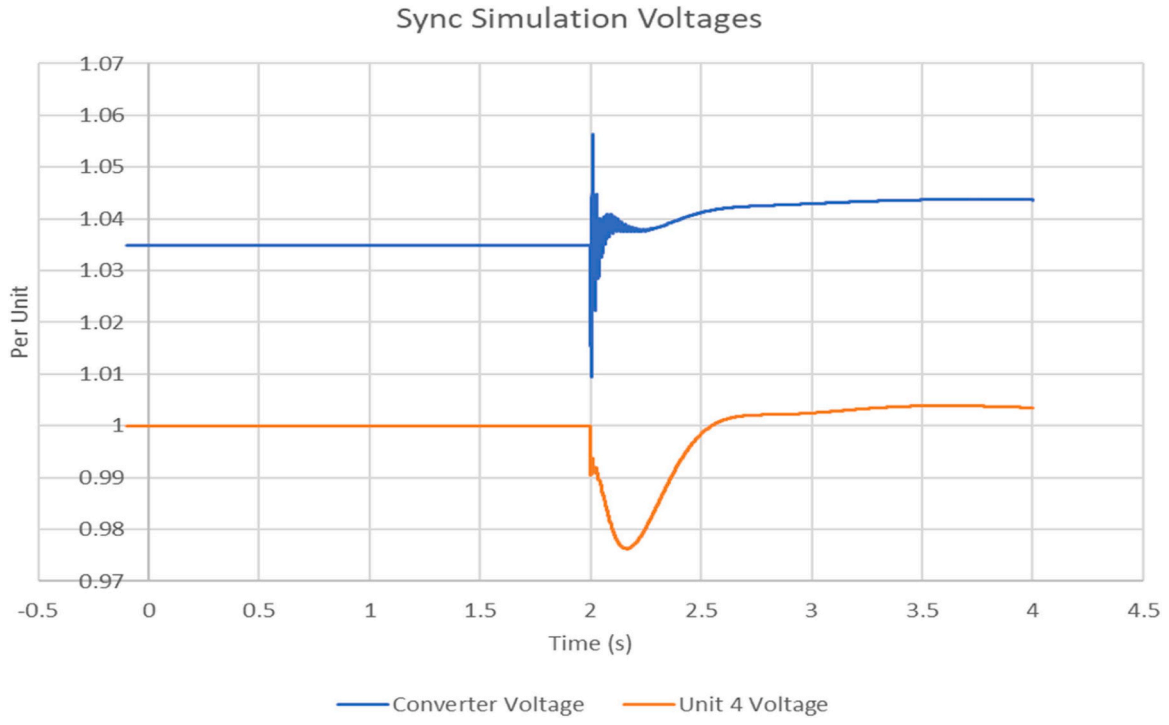

Fig. 10. Sync voltage simulation results.

black starting the unit starting at any hour of the year. There is a high level of variability in the energy requirements depending on the time of day the start is initiated. Taking the average battery energy consumption at each hour of the day as a measure, the optimal hour to initiate a black start is 11 PM. (Fig. 14)

Relaxing the requirement of 100 % capability for every hour of the

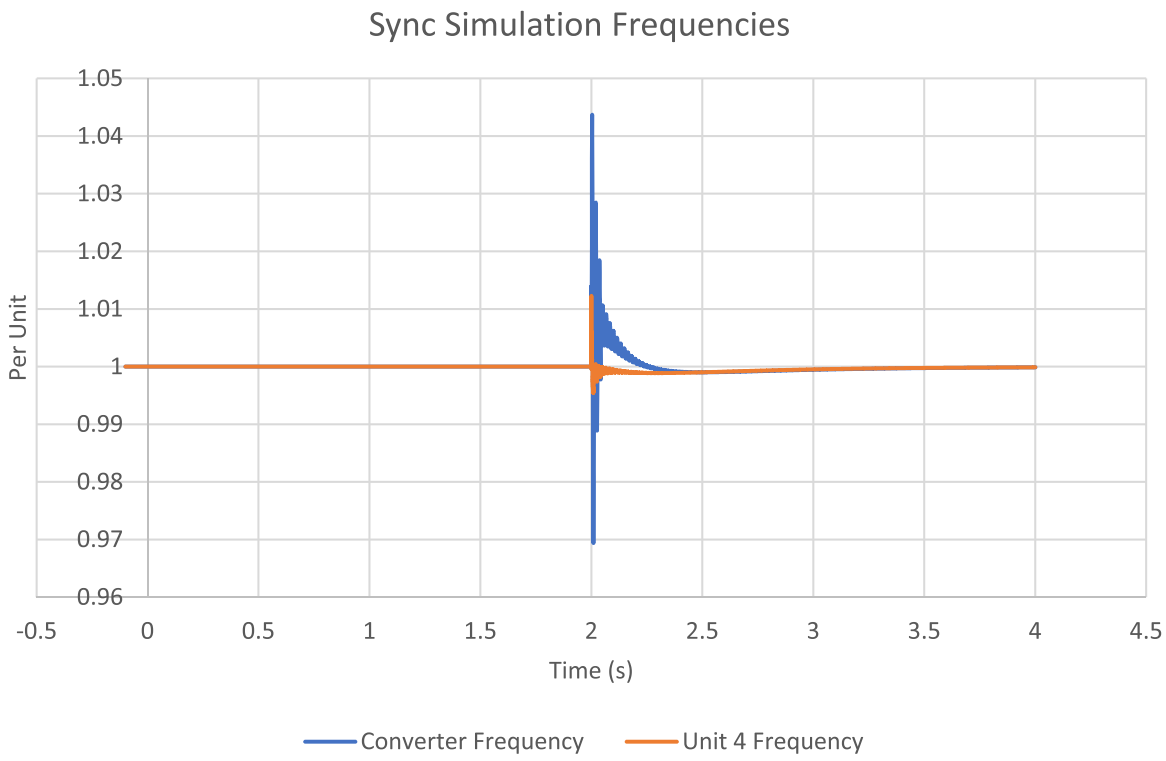

Fig. 11. Sync frequency simulation results.

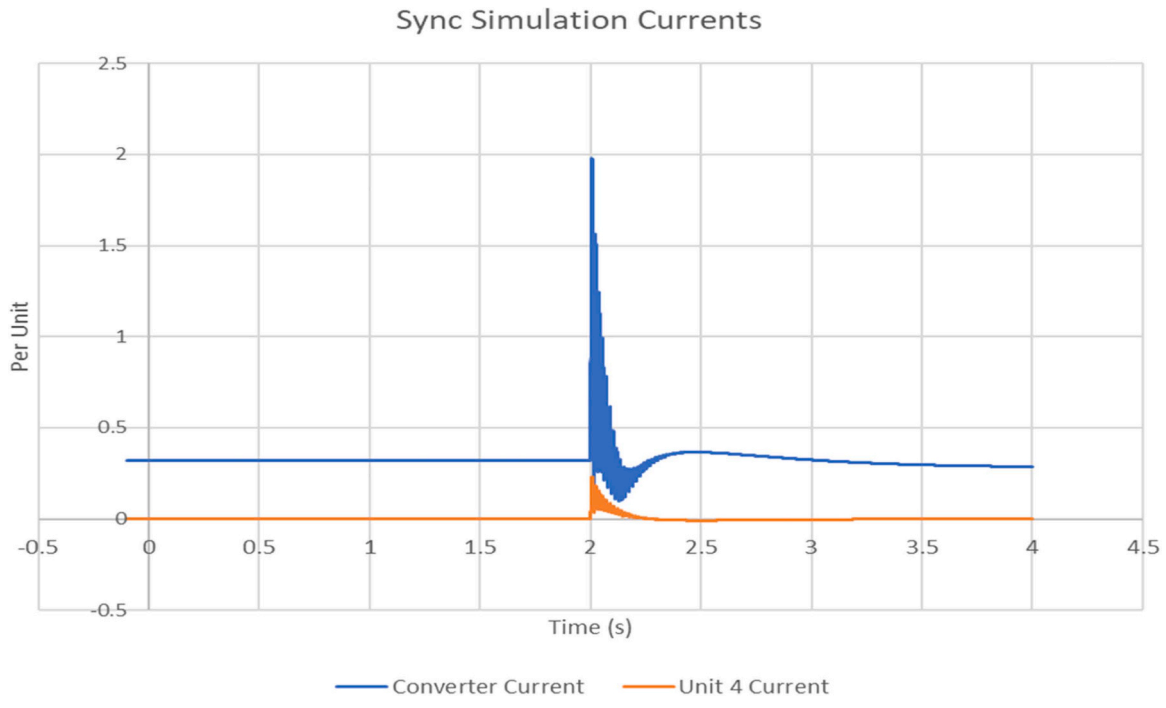

Fig. 12. Sync current simulation results.

year, the stored energy required to start up the unit can be reduced. Assuming a time window of 5 days to initiate a black start reduces the stored energy requirement by 34 % to 155 MWhr per battery plant. (Fig. 15)

4.4. *Energy benefits-solar system installations*

Three models are developed to compare the energy benefits of the solar installation:

- Base case
- Solar install
- Reduce coal fuel with solar

The base case model is configured with the synchronous generator generating and the solar/battery installation is disconnected. A year

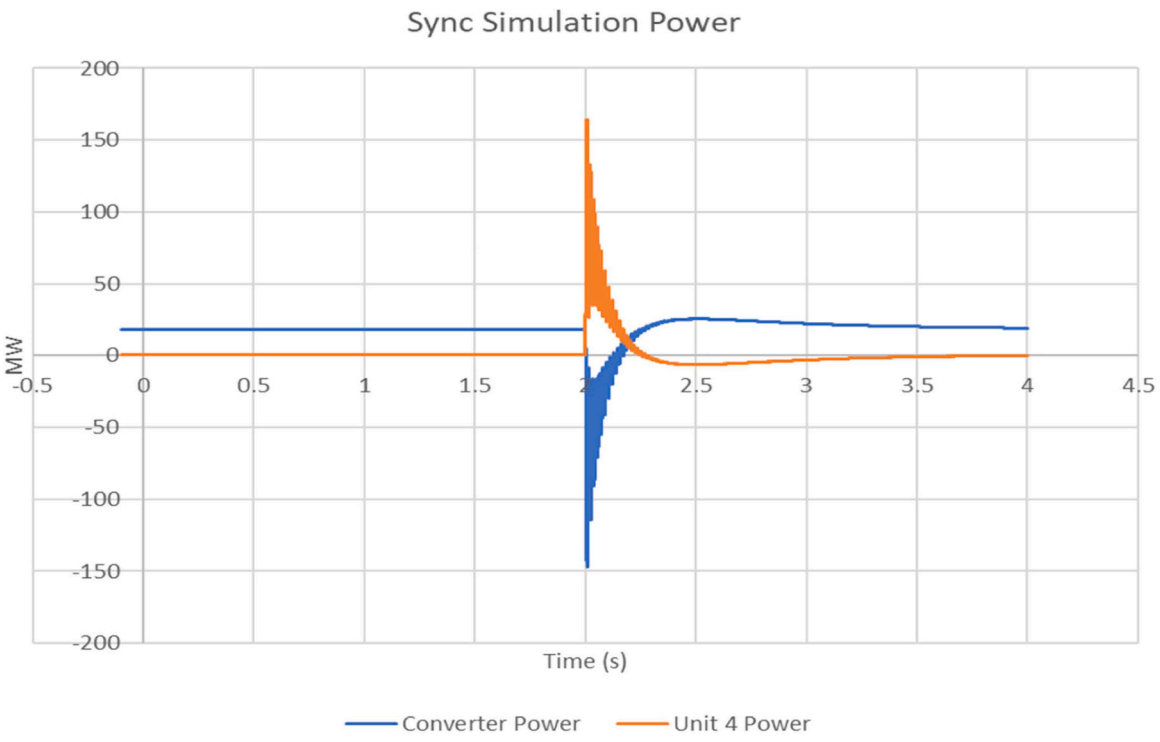

Fig. 13. Sync power simulation results.

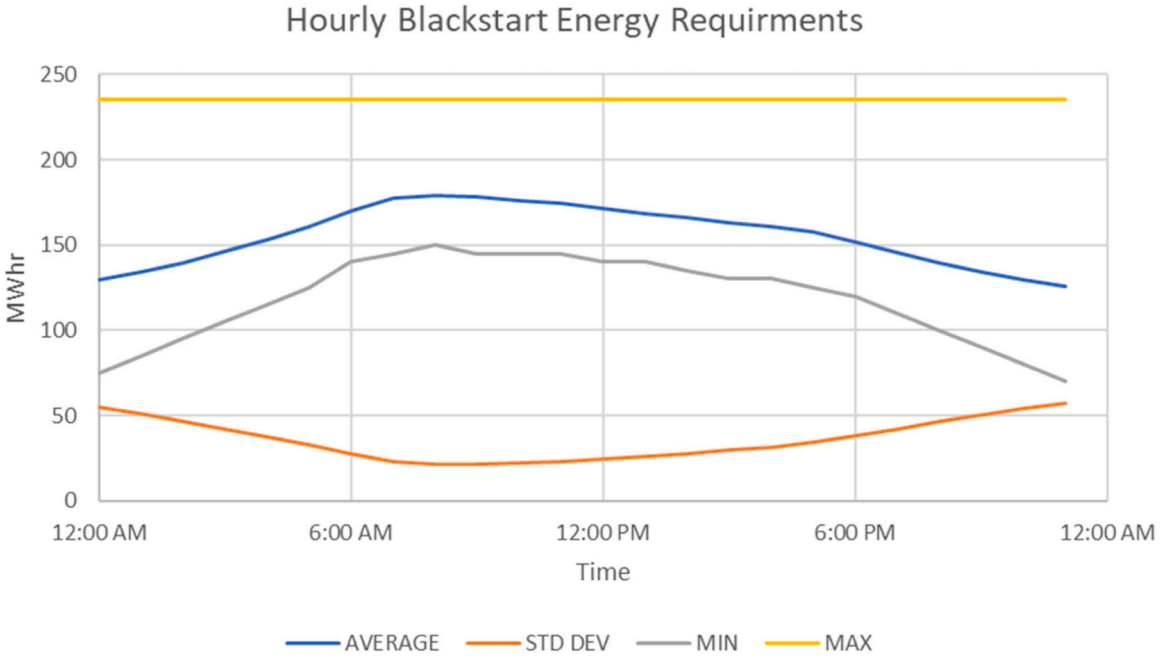

Fig. 14. Black start energy requirements.

(2022) of 1 minute power data is used for the auxiliary loads as well as unit dispatch. The solar install model also has the synchronous generator generating, but also has the solar/battery plants connected and generating. The same base case power data is used. In addition, the hourly solar irradiation data from the 2020 NREL Typical Metrological Year database [27] is used in the model to calculate photovoltaic generation. The reduce coal fuel with solar model is identical to the solar install model, except for the power data used. This model constrains the point of connection (POC) output to that of the base case. The solar generation reduces the synchronous generation to keep the export the same as the base case. But this reduction is constrained by the synchronous generator's minimum operating output of 240 MW.

The two 35 MW solar plants produced 81,941 MWhr for the year. Using the average US price of electricity ($0.111/kWhr)[28], this equates to about $9.1 million. The unit output increased by 2.5 %. The reduce coal fuel simulation calculates a reduction of 47,607 MWhr or a 1.5 % reduction in synchronous generator output. This reduces the amount of coal burned over a year by an estimated 21,100 metric tons, while also exporting an additional 34,334 MWhr of energy ($3.8 million) from the solar plants.(Fig. 16)

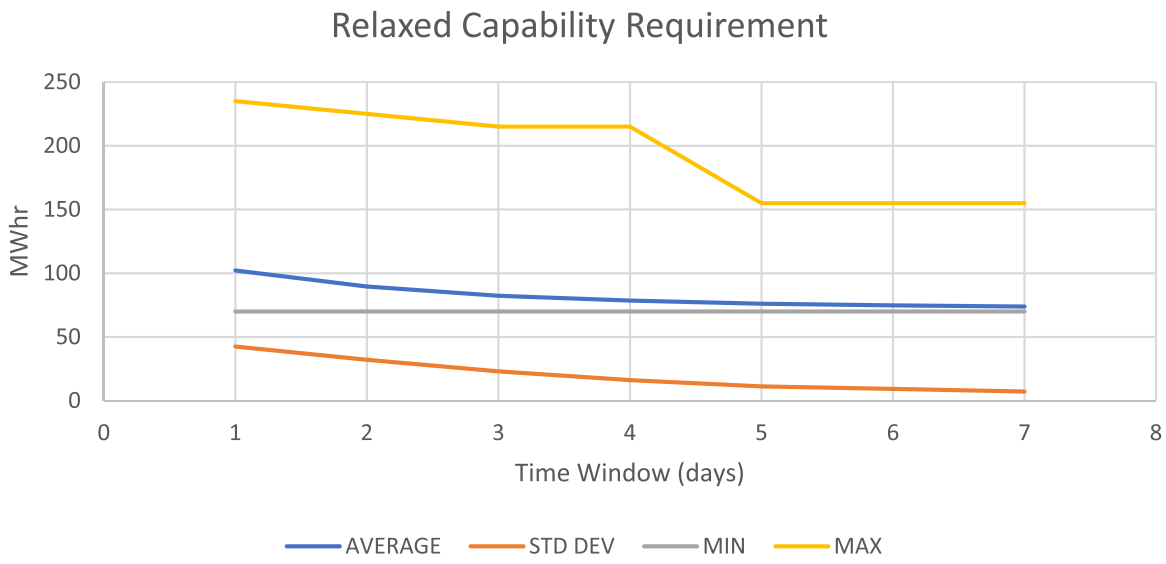

Fig. 15. Black start relaxed start requirements.

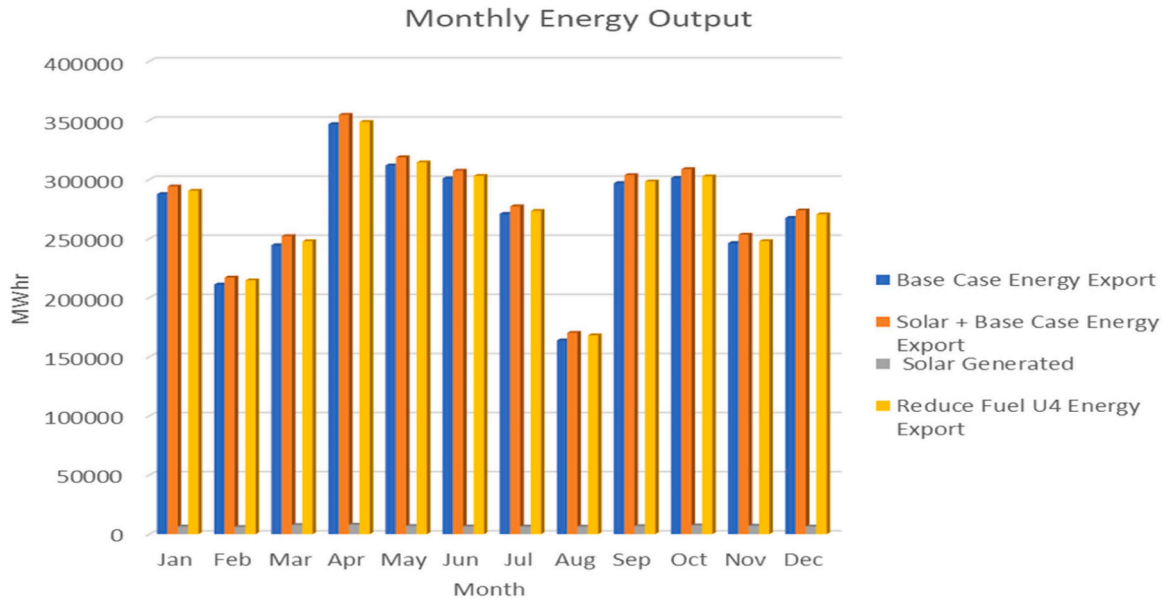

Fig. 16. Monthly Energy Output.

5. Conclusions

The objective of this paper is to model and simulate integration of solar power and battery to an existing fossil fuel power plant to reduce fuel burn and provide black-start capability. The performance of the proposed methodology is demonstrated through detailed simulations and analyses. Dynamic simulations show the unit can be black started utilizing a grid forming inverter with battery energy storage. The simulations demonstrate the ability of the grid forming inverters to start the largest motor loads required by the unit during run up. It is also shown that the synchronous generator can synchronize with the converter driven microgrid while maintaining grid stability. Additional analysis determines the stored energy requirements of the battery system. Finally, it quantifies the savings of energy and reduced fuel benefits with hybridization of energy resources. The proposed management algorithm faces two primary drawbacks. Firstly, there are challenges in tuning the droop controls for motor starts and generator synchronization. Ideally, these parameters should be dynamically optimized based on system conditions and the equipment being brought online, a topic highlighted for future research in this field. Secondly, the LSTM regression model employed to calculate the reduced auxiliary load relies on one year of data. Future research aims to address this limitation by updating the model in real-time as new load data becomes available.

CRediT authorship contribution statement

Jahangir Hossain: Writing – review & editing, Supervision, Investigation, Conceptualization. **Michael Beck:** Writing – original draft, Validation, Methodology, Conceptualization.

Declaration of Competing Interest

The authors declare that they have no known competing financial interests or personal relationships that could have appeared to influence the work reported in this paper.

Data Availability

Data will be made available on request.

Appendix A

PA Motor parameters

Voltage	6.6kv
Rated mechanical Power	1268 kW
Nominal Frequency	60 Hz
Rated Speed	1786 rpm
Pole Pairs	2
Locked Rotor current	5.48 pu
Locked rotor torque	.69 T/Tn
Torque at stalling point	2.28 T/Tn

ID Motor parameters

Voltage	6.6kv
Rated mechanical Power	7271 kW
Nominal Frequency	60 Hz
Rated Speed	716 rpm
Pole Pairs	5
Locked Rotor current	6.5 pu
Locked rotor torque	.9 T/Tn
Torque at stalling point	2.25 T/Tn

BESS GFM converter settings

Setting	PA Motor Start	ID Motor Start	Generator Sync
P droop	0.01 pu	0.01 pu	0.01 pu
Q droop	0.01 pu	0.01 pu	0.01 pu
Low-pass filter cut-off	60 Hz	72 Hz	60 Hz
Virtual R	0.01 pu	0.0006 pu	0.01 pu
Virtual X	0.01 pu	0.006 pu	0.01 pu
Over-current limit	1.01 pu	1.01 pu	1.01 pu
Proportional R factor	2 pu	8 pu	2 pu
Proportional X factor	2 pu	8 pu	2 pu

References

[1] H.R. a M. Roser. Electricity Mix [Online] Available: ⟨https://ourworldindata.org/energy'⟩.

[2] Australian Energy Martket Operator. (2020). Renewable Integration Study: Stage 1 report. [Online] Available: ⟨https://www.aemo.com.au/-/media/files/major-publications/ris/2020/renewable-integration-study-stage-1.pdf⟩.

[3] Y.T. Shah, Hybrid power: generation, storage, and grids (Sustainable energy strategies), CRC Press, Boca Raton, FL, 2021.

[4] B. Matich. (2021, 24 March 2021) The race that stores the nation – AGL green lights 250 MW Torrens Island battery. PV Magazine. Available: ⟨https://www.pv-magazine-australia.com/2021/03/24/the-race-that-stores-the-nation-agl-green-lights-250-mw-torrens-island-battery/⟩.

[5] B. PEACOCK. (2021, 10 August 2021) World's largest 'grid forming' battery to begin construction near Adelaide. PV Magazine. Available: ⟨https://www.pv-magazine-australia.com/2021/08/10/worlds-largest-grid-forming-battery-to-begin-construction-near-adelaide/⟩.

[6] Y.D. b Mohammad Alsmadi a and A. A.-S. c, Utilizing PV system for auxiliary energy demand in conventional power plant, Int. J. Therm. Environ. Eng. vol. 14 (2) (2017) 119–124.

[7] AM Solar - Jordan. Nebras Power. ⟨https://nebras-power.com/assets/listing/am-solar⟩.

[8] A. Tbaileh *et al.*, "Optimal Power System Black start using Inverter-Based Generation," 2021: IEEE, doi: 10.1109/pesgm46819.2021.9638043. [Online]. Available: ⟨https://dx.doi.org/10.1109/pesgm46819.2021.9638043⟩.

[9] Q. Nguyen, M.R. Vallem, B. Vyakaranam, A. Tbaileh, X. Ke, and N. Samaan, "Control and Simulation of a Grid-Forming Inverter for Hybrid PV-Battery Plants in Power System Black Start," 2021: IEEE, doi: 10.1109/pesgm46819.2021.9637882. [Online]. Available: ⟨https://dx.doi.org/10.1109/pesgm46819.2021.9637882⟩.

[10] H. Jain, G.-S. Seo, E. Lockhart, V. Gevorgian, and B. Kroposki, "Blackstart of Power Grids with Inverter-Based Resources," 2020: IEEE, doi: 10.1109/pesgm41954.2020.9281851. [Online]. Available: ⟨https://dx.doi.org/10.1109/pesgm41954.2020.9281851⟩.

[11] J. Sawant, G.-S. Seo, and F. Ding, "Resilient Inverter-Driven Black Start with Collective Parallel Grid-Forming Operation: Preprint," presented at the Conference: Presented at the 2023 IEEE Conference on Innovative Smart Grid Technologies North America (ISGT NA), 16-19 January 2023, Washington, D.C., United States, 2022. [Online]. Available: ⟨https://www.osti.gov/biblio/1906867⟩. ⟨https://www.osti.gov/servlets/purl/1906867⟩.

[12] E. Fix, A. Banerjee, U. Muenz, and G.-S. Seo, "Investigating Multi-Microgrid Black Start Methods Using Grid-Forming Inverters: Preprint," presented at the Conference: Presented at the 2023 IEEE Conference on Innovative Smart Grid Technologies North America (ISGT NA), 16-19 January 2023, Washington, D.C., United States, 2023. [Online]. Available: ⟨https://www.osti.gov/biblio/1922187⟩. ⟨https://www.osti.gov/servlets/purl/1922187⟩.

[13] A.A.A. Alahmadi, et al., Hybrid wind/PV/battery energy management-based intelligent non-integer control for smart DC-microgrid of Smart University, IEEE Access vol. 9 (2021) 98948–98961, https://doi.org/10.1109/ACCESS.2021.3095973.

[14] Y. Sahri, et al., Energy management system for hybrid PV/wind/battery/fuel cell in microgrid-based hydrogen and economical hybrid battery/super capacitor energy storage, Energies vol. 14 (18) (2021) 5722, https://doi.org/10.3390/en14185722.

[15] Y. Belkhier, A. Oubelaid, Novel design and adaptive coordinated energy management of hybrid fuel-cells/tidal/wind/<scp>PV</scp> array energy systems with battery storage for microgrids, Energy Storage vol. 6 (1) (2024), https://doi.org/10.1002/est2.556.
[16] N. Khosravi, et al., A novel control approach to improve the stability of hybrid AC/DC microgrids, 2023/08/15/, Appl. Energy vol. 344 (2023) 121261, https://doi.org/10.1016/j.apenergy.2023.121261.
[17] A. Peña Asensio, S. Arnaltes Gómez, J.L. Rodriguez-Amenedo, Black-start capability of PV power plants through a grid-forming control based on reactive power synchronization, 2023/03/01/, Int. J. Electr. Power Energy Syst. vol. 146 (2023) 108730, https://doi.org/10.1016/j.ijepes.2022.108730.
[18] I.C. Report, Dynamic models for steam and hydro turbines in power system studies, IEEE Trans. Power Appar. Syst. vol. PAS-92 (6) (1973) 1904–1915.
[19] S. Rangnekar, Development of state space model and study of performance characteristics of digital based excitation control system ST4B with single machine connected to infinite bus, IEEE, doi: 10.1109/cca.1999.801187. [Online]. Available: ⟨https://dx.doi.org/10.1109/cca.1999.801187⟩.
[20] "IEEE Recommended Practice for Excitation System Models for Power System Stability Studies," doi: 10.1109/ieeestd.2016.7553421.
[21] M. Swierczynski, D.-I. Stroe, A.-I. Stan, R. Teodorescu, and S.K. Kaer, "Investigation on the Self-discharge of the LiFePO<inf>4</inf>/C nanophosphate battery chemistry at different conditions," 2014: IEEE, doi: 10.1109/itec-ap.2014.6940762. [Online]. Available: ⟨https://dx.doi.org/10.1109/itec-ap.2014.6940762⟩.
[22] A. Wagner, Photovoltaik Engineering, Springer, 2009.
[23] S. Eberlein, K. Rudion, Small-signal stability modelling, sensitivity analysis and optimization of droop controlled inverters in LV microgrids, Int. J. Electr. Power Energy Syst. vol. 125 (2021) 106404, https://doi.org/10.1016/j.ijepes.2020.106404.
[24] A.D. Paquette, D.M. Divan, Virtual impedance current limiting for inverters in microgrids with synchronous generators, IEEE Trans. Ind. Appl. vol. 51 (2) (2015) 1630–1638, https://doi.org/10.1109/tia.2014.2345877.
[25] "Researchers at Federal Technological University of Parana Release New Data on Renewable Energy (Operational and Control Approach for Pv Power Plants To Provide Inertial Response and Primary Frequency Control Support To Power System Black-start)," Ecology, Environment & Conservation, p. 1178, 2021.
[26] W. Yan, Q. Hong, D. Liu, and A. Dyśko, Feasibility studies on black start capability of distributed energy resources, 2021: Institution of Engineering and Technology, doi: 10.1049/icp.2021.2257. [Online]. Available: ⟨https://dx.doi.org/10.1049/icp.2021.2257⟩.
[27] NREL. 2020 Typical Meteorological Year (TMY) Solar Radiation.
[28] U.S. Department of Energy, Electr. Power Annu. 2021. (2022).